Journal of Alloys and Compounds 506 (2010) L22–L24

Contents lists available at ScienceDirect

Journal of Alloys and Compounds

journal homepage: www.elsevier.com/locate/jallcom

Letter

Thermochromic property of $La_{0.8}Sr_{0.2}MnO_3$ thin-film material sputtered on quartz glass

Chunhua Wu[a,*], Jiawen Qiu[b], Jiebing Wang[a], Min Xu[a], Lanxi Wang[a]

[a] National Key Laboratory of Science and Technology on Surface Engineering, Lanzhou Institute of Physics, 97 Weiyuan Road, Lanzhou 730000, China
[b] Research and Development Centre, China Academy of Space Technology, 104 Youyi Road, Beijing 100094, China

ARTICLE INFO

Article history:
Received 12 September 2009
Received in revised form 13 July 2010
Accepted 14 July 2010
Available online 22 July 2010

Keywords:
Thermochromic
Thin film
Variable emittance
Magnetron sputtering

ABSTRACT

$La_{0.8}Sr_{0.2}MnO_3$ (LSMO) thin films have been grown on quartz glass at room temperature by sputtering LSMO compound and followed by post-annealing. Crystalline structure, infrared reflectance spectrum and temperature dependent of infrared emittance were investigated. The result indicates that there exists a significant transition in thermal emittance over the temperature range between 170 K and room temperature, which could potentially be explored for smart spacecraft thermal radiator application.

1. Introduction

Spacecrafts are subjected to large environment temperature fluctuation from −150 to +150 °C. In order to maintain all the component of spacecraft within their respective temperature limitation, an efficient thermal-control system is indispensable. In recent years, variable-emittance materials have attracted more attention for its superiority in deep space exploration application. These materials can automatically adjust its infrared emittance to high or low in response to variations in the thermal load and environmental temperature [1]. There has been great interest in thermochromic materials $La_{1-x}Sr_xMnO_3$ (LSMO) and $La_{1-x}Ca_xMnO_3$ (LCMO). These materials are perovskite-type manganese oxides and undergo the metal to insulator (M–I) transition at Curie temperature once up-warmed in certain doping concentration [2]. In general, metals are usually less emissive than insulators, so the M–I transition leads to a big increase in infrared emittance. Tachikawa and co-workers reported the smart radiation device (SRD) based on $La_{0.825}Sr_{0.175}MnO_3$ ceramic tile which can controls the heat flow in response to its own temperature without electrical and mechanical parts [3]. The tunability of infrared emittance of this material between 173 and 373 K reaches to 0.37. Also the structure, infrared absorption and temperature dependence of normal emittance of bulk $La_{1-x}A_xMnO_3$ (A = Sr and Ca) in 3–5 and 8–14 μm were studied [4] but the fabrication process of the ceramic tile is inconvenient. As a result of this, variable-emittance radiator based on (La, Sr) MnO_3 thin films has been developed by Sol–Gel method [5]. As a solution coating method, the Sol–Gel method inevitably results pollution, and the issues of uniformity and cracking of the coating should be take into account. Jiang et al. synthesized $La_{0.825}Sr_{0.175}MnO_3$ and $La_{0.7}Sr_{0.3}MnO_3$ thin films by pulse laser deposition on single crystal Si and a metal substrate, and the $La_{0.7}Sr_{0.3}MnO_3$ thin-film exhibits more significant transition (0.3) in their thermal emittance (200–400 K) [6]. But for its lack of uniform on thickness, the transition in thermal emittance occurs over relatively wide temperature range.

In this article, attempt is made to synthesis the LSMO thin films by magnetron sputtering for its superiority in good adhesive and large-area deposition. We focused on the performance of thin films for its thermal-control application, and using two-phase phenomenological mode to explain the temperature dependence of emittance. Further investigations on emittance vs. grain size and temperature will be summarized in our next study.

2. Experimental

Thin films were deposited on quartz glass substrate by using DC magnetron sputtering system from nominal composition $La_{0.8}Sr_{0.2}MnO_3$ compound target. These films were sputtered at room temperature in a mixture gas of Ar and O_2, and followed by post-annealing at 700 °C at air atmosphere. The structure of samples was characterized by Philip X-ray diffractometer using Cu Kα radiation (λ = 0.154056 nm). The composition was checked by X-ray energy disperse spectral (EDS). Infrared reflectance spectrum was measured by SYSTEM2000 infrared spectrometer of PerkinElmer Ltd. Temperature dependent of total hemispherical emittance (ε_H) was measured in liquid nitrogen cooled vacuum chamber by a steady state calorimetric method [7].

* Corresponding author. Tel.: +86 931 4585515; fax: +86 931 8265391.
E-mail address: 451810583@qq.com (C. Wu).

0925-8388/$ – see front matter © 2010 Elsevier B.V. All rights reserved.
doi:10.1016/j.jallcom.2010.07.112

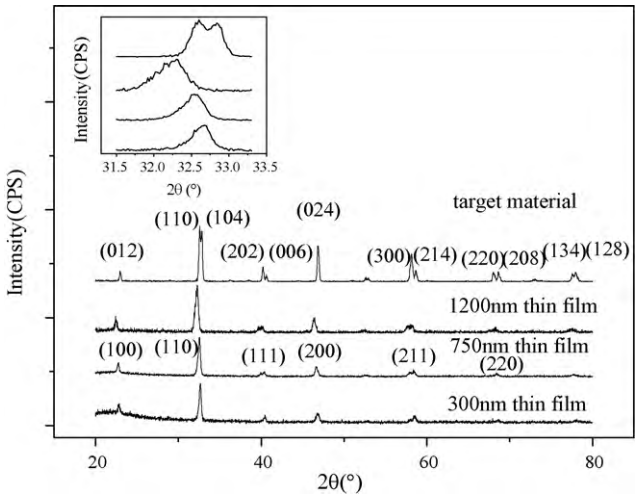

Fig. 1. XRD patterns of bulk material and thin films.

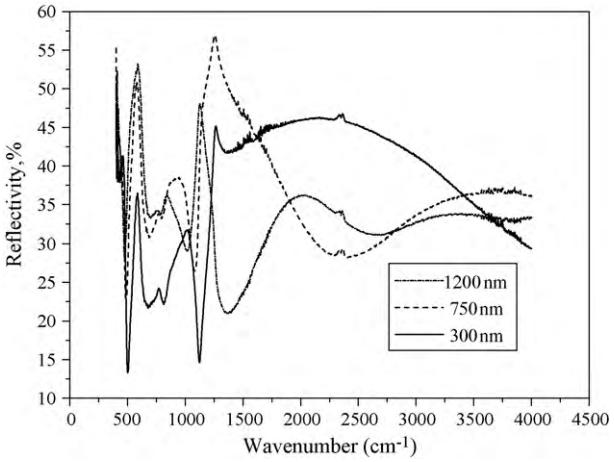

Fig. 2. Spectral reflectance of thin films samples.

3. Result and discussion

Fig. 1 shows the XRD patterns of target material and 3 thin-film samples. All samples are perovskite phase with polycrystalline structure. Target material has a hexagonal lattice, whereas thin films are indexed as pseudocubic structure. The structures of 300, 750 nm thin films are similar to that of 1200 nm thin film, except for a broad substrate amorphous diffraction peaks at lower diffraction angle. The composition analysis checked by X-ray EDS showed the target and the thin-film sample have a comparable stoichiometry within the sensitivity limit of EDS (not shown here). It suggested the structure difference is not caused by the composition discrepancy. For the parent material $LaMnO_3$, it is cubic structure. However, for the Sr doped bulk $La_{1-x}Sr_xMnO_3$, the crystal is usually distorted into orthorhombic or hexagonal structure which is dependent on the doping concentration x. The diffraction peaks shift towards to high-angle direction (seen clearly from the inset) with the decrease of thickness indicating the lattice constant becomes smaller, which is favors of enhancement of double exchange mechanism and Curie temperature. This is proved by variable temperature emittance in Fig. 3. Lattice constant of 3 thin films samples, in the ascending order of thickness, calculated by XRD data is ≈0.3865, 0.3875 and 0.3882 nm. The results show the thinner film has a lattice constant close to distortion-free $LaMnO_3$. Compared to target material, thin film is easier to relax to reduce the distortion, so its structure is close to cubic structure as $LaMnO_3$, whereas the distortion in bulk material cannot be eliminated, it usually distorted into hexagonal structure. The mechanism for relaxation is perhaps different from that of films grown on single crystal substrates [8].

The infrared (IR) reflectance spectrum of the films is shown in Fig. 2 in the 400–4000 cm^{-1} range. These features of the obtained reflectance spectra of our polycrystalline thin-film samples agree well with those obtained from polycrystal. Reflectivity curve shows obvious phonon peak around the position of 600 cm^{-1} corresponding to Mn–O stretching mode [3]. For the three thin films samples, the stretching mode peaks are respectively located at 587, 581 and 589 cm^{-1}. In thin-film samples, there are still notable phonon peaks located between 840 and 1030 cm^{-1}, which only appeared at high temperature, and they are obviously affected by conductive states of the samples. At the high-wavenumber region higher than 1100 cm^{-1}, there is a contribution of substrate to the high reflectivity around 1120 cm^{-1}.

Thermal radiation property of thin films (shown in Fig. 3) shows all samples have low emittance in the low-temperature range, and have higher emittance in the high-temperature range to 300 K. In the entire temperature range, the emittance monotonously increases with temperature increase. Large emittance at high temperature is necessary to be large to meet the requirement to dissipate the waste heat to external space more efficiently, and the variation of emittance needs to be tuned as large as possible. Among the three thin-film samples, the emittance of 300 nm thin film varies from 0.54 at 175 K to 0.73 at 300 K ($\Delta\varepsilon_H = 0.19$), and the 750, 1200 nm thin films, show a net emittance change of 0.14 (174–294 K) and 0.17 (181–292 K), respectively. The transition temperature (T_p), approximately determined from the inflection point of ε_H–T curve, is in the range of 200–240 K for the 750 and 1200 nm thin films, in contrast with transition temperature happened in the range of 220–250 K for the 300-nm film. Except for thickness, the deposition and annealing conditions of the three samples are identical. The deviation in transition temperature might be attributed to the difference of oxygen content in the films obtained in the annealing process.

According to electromagnetic theory, the penetrate strength of incident radiation energy becomes $(1/e)^n$ after n times skin depths [9]. Thin film with several skin depths is sufficient to ensure the infrared property has no distinguished difference with bulk material. Because 1200-nm film has a comparable room-temperature (RT) emittance to bulk material (refers to thickness dependent of RT emittance in the insets of Fig. 3), the average skin depth is estimated to be several hundreds of nanometers close to the thickness of the two thinner films. It is known the substrate is not a phase

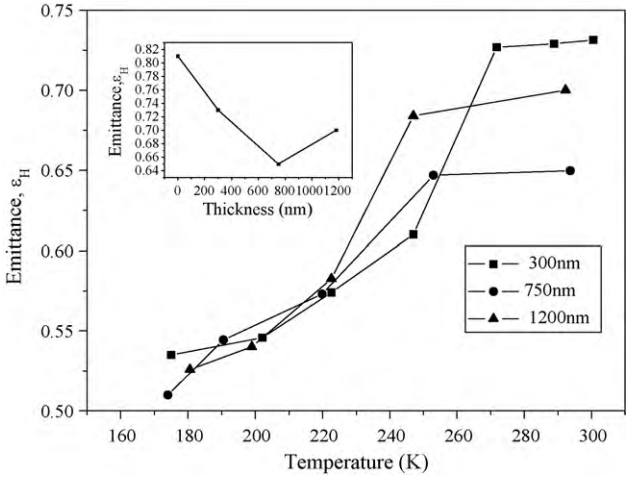

Fig. 3. Temperature dependence of infrared emittance.

material, the emittance changes slightly with temperature variation (less than 0.02). As a result of this, the emittance of substrate is also high (close to 0.81) from low temperature to high temperature. This consequently leads to thin film with thickness smaller than skin depth has a high emittance both at high temperature and low temperature. With increase of thickness, the intrinsic infrared property dominates over the substrate effect. For the 1200 nm film, its room-temperature emittance reaches to 0.70 which is close to 0.74 of that of LSMO bulk material unpolished.

Note that the transition temperature of film materials (except for epitaxial film) is often far lower than that of bulk materials [10], and also the variation of emittance of thin film between 373 and 173 K is not large as that of ceramic bulk material. This is probably a consequence of phase separation [11,12]. Since 1950s, the properties of LSMO materials have been explained by double exchange effect and Jahn–Teller effect [13,14]. Until recent years, phase separation mode has been used to explain the nature of metal to insulator transition at certain doping concentration and also temperature-induced phase change. The phenomenon of phase separation corresponds to the simultaneous existence of subphase of metal and insulator. As temperature increases, part of the metallic phase gradually turns into insulator phase. Towards a certain high temperature, the insulator phase spreads in all the material. Based on the above analysis, temperature dependent of emittance can be qualitatively described by phase separation scenario of metal and insulator. On the assumption that ε_H is totally due to the emittance of metal phase ($\varepsilon_{H,M}$) and insulator phase ($\varepsilon_{H,I}$) as $\varepsilon_H = \varepsilon_{H,M} \times f + \varepsilon_{H,I} \times f'$ where f and f' are the volume fraction of metal and insulator phase. Tang et al. use a two-energy Boltzmann distribution to fitting the experiment result of ε_H vs. T with the above expression, but the fitting method is lack of consideration of the temperature dependent variation on $\varepsilon_{H,M}$ and $\varepsilon_{H,I}$, and not giving the relations of grain size to energy level [15]. Here, we mainly make a disclosure of the essence of phase separation on the temperature dependent of emittance. Thin-film material usually grows at 700 °C with small crystalline grain size about 35 nm estimated by Scherrer formula using XRD data, whereas bulk ceramic material sintered at around 1300 °C has a large grain size to micron scale observed by SEM. The double exchange interaction, which is often used to explain the intrinsic conductive behavior of perovskite manganese oxide, is weaker in the grain surfaces than in the grain cores due to large number of dangling bonds existing in the surface. For this reason, grain boundary is regarded as insulator phase; on the contrary, the crystalline grains can be treated as metal phase. In view of assumption of the ε_H, the emittance is determined by the respective emittance value of crystalline grain phase, grain boundary phase and the contribution proportion of the two phases. Here we assume the fraction of f and f' is unchanged, but $\varepsilon_{H,M}$ and $\varepsilon_{H,I}$ are dependent on temperature. Compared to crystalline grain, grain boundary has a low ordering temperature. With increase of temperature, the chaos around grain boundary is more distinct, i.e., the material is more insulating, consequently leading to gradual increase of emittance. Unlikely, the ordering temperature of crystalline grain is higher enough than that of grain boundary. Although the crystalline grain phase is also becoming towards insulator as temperature increase, it is still in metallic phase in a wide temperature range far below than grain ordering temperature. The gross effect is the emittance is monotonically gradually increased when the temperature is on warming. When the temperature is close to the ordering temperature of crystalline grain, in accordance with percolation picture, the insulator domains form infinite clusters and impenetrate the whole sample, thus the materials turn into almost complete insulator which leads to emittance of thin film increases significantly. With grain growth, f' term reduces and f term increases. As for bulk material, the grain size is in micron scale, so the f factor becomes prominent. That means the boundary almost disappears with a minimum of insulator phase. Therefore the emittance depends on grain boundary is very weak and the emittance variation with temperature change is small bellow the ordering temperature of metal phase; only at the grain crucial temperature, intrinsic body phase metal–insulator transition occurs with a great change in emittance in a relatively narrow temperature range.

4. Conclusions

Thermochromic films were successfully synthesized on quartz glass by sputtering technique at room temperature and post-annealing. Microstructure characterization indicates that the films are perovskite phase with polycrystalline structure. The infrared reflectance spectrum shows intrinsic phonon structure which is corresponds to Mn–O octahedron stretching mode. Measurement of total hemispherical emittance was made and the results indicate that the films exhibit significant transition in thermal emittance over the temperature range between 170 and 300 K, which is attractive to be used for smart thermal control of spacecraft. Thickness dependence of emittance is discussed, and the results show the skin depth of thin films is several hundreds nanometers, also temperature dependent of emittance based on two-phase mode is qualitatively explained which is consistent with experimental observation. The relation of grain size to the critical temperature of grain boundary is an academic interest needed to be paid more attention. However, until now, to our acknowledge, any works on the effect of grain boundary to critical temperature of polycrystalline material and the formation of insulator phase with changing temperature have not been done.

Acknowledgement

We thank Dr. Chunfang Wu for valuable discussions and assistance.

References

[1] T.D. Swanson, G.C. Birur, Appl. Therm. Eng. 23 (2003) 1055.
[2] A. Urushibara, Y. Moritomo, T. Arima, A. Asamitsu, G. Kido, Y. Tokura, Phys. Rev. B 51 (1995) 14103.
[3] K. Shimazaki, S. Tachikawa, A. Ohnishi, Y. Nagasaka, Int. J. Thermophys. 22 (2001) 1549.
[4] X.M. Shen, G.Y. Xu, C.M. Shao, C.W. Chen, J. Alloys Compd. 479 (2009) 420.
[5] Y. Shimakawa, T. Yoshitake, Y. Kubo, T. Machida, K. Shinagawa, A. Okamoto, et al., Appl. Phys. Lett. 80 (2002) 4864.
[6] X. Jiang, M. Soltani, D. Mishikinis, M. Chaker, D. Nikanpour, Proceedings of the 10th ISMSE & the 8th ICPMSE, Collioure, France, 2006.
[7] K. Fukuzawa, A. Ohnishi, Y. Nagasaka, Int. J. Thermophys. 23 (2002) 319.
[8] W.S. Tan, H.P. Hu, K.M. Deng, X.S. Wu, Q.J. Jia, J. Gao, J. Alloys Compd. 491 (2010) 545.
[9] F. wooten, Optical Properties of Solids, Academic Press, San Diego, 1972.
[10] S.Y. Yang, W.L. Kuang, Y. Liou, W.S. Tse, S.F. Lee, Y.D. Yao, J. Magn. Magn. Mater. 268 (2004) 326.
[11] G. Li, H.D. Zhou, S.J. Feng, X.J. Fan, X.G. Li, G.D. Wang, J. Appl. Phys. 92 (2002) 1406.
[12] J. Burgy, M. Mayr, V. Martin-Mayor, A. Moreo, E. Dagotto, Phys. Rev. Lett. 87 (2001) 2772021.
[13] C. Zenner, Phys. Rev. 82 (1951) 403.
[14] A.J. Millis, P.B. Littlewood, B.I. Shraiman, Phys. Rev. Lett. 74 (1995) 5144.
[15] G.C. Tang, Y. Yu, Y.Z. Cao, W. Chen, Solar Energy Mater. Solar Cell 92 (2008) 1298.